Piezotronic effect on Rashba spin-orbit coupling based on $MAPbI_3$/ZnO heterostructures

Laipan Zhu[1,2] and Zhong Lin Wang*[,1,2,3]

1 CAS Center for Excellence in Nanoscience, Beijing Key Laboratory of Micro-nano Energy and Sensor, Beijing Institute of Nanoenergy and Nanosystems, Chinese Academy of Sciences, Beijing 100083, P. R. China

2 School of Nanoscience and Technology, University of Chinese Academy of Sciences, Beijing 100049, P. R. China

3 School of Material Science and Engineering, Georgia Institute of Technology, Atlanta, Georgia 30332, USA

*E-mail: zhong.wang@mse.gatech.edu

Abstract

Rashba spin-orbit coupling (SOC) is a core issue in semiconductor spintronics, which allows the manipulation of electron spin through electric field rather than an external magnetic field, revealing bright prospect for advanced electronic devices with ultra-high speed and integration. On the other side, the emerging piezotronic effect is the born characteristics for many semiconductors that have non-central symmetric structure, such as ZnO and GaN. Here, we design three heterostructure devices, based on piezoelectric p-type $(CH_3NH_3)PbI_3$ single crystal and n-type wurtzite-structured ZnO thin-film, to theoretically study on how the piezotronic effect can effectively work on the Rashba spin-orbit coupling. Benefiting from a large piezoelectric charges at the interface when a vertical strain is applied, a high concentration of two-dimensional electron gas is induced in the plane of heterostructure, which can tune the built-in electric field at the interface and further manipulate the Rashba SOC. With the increase of pressure, both Rashba parameter and spin splitting are found to first vanish and then increase linearly for ZnO with doping density of 10^{15} and 10^{16} cm^{-3}. This work provides an insight of manipulating electron spins via the introduction of piezo-charges, showing great application potential of piezotronic effect in tuning spintronic devices.

Keywords

Rashba spin-orbit coupling, ZnO, perovskite, piezotronic effect, piezo-charges

Semiconductor spintronics is developing rapidly due to its bright prospect in advanced electronic devices with ultra-high speed, ultra-high integration and ultra-low power consumption.[1,2] Spin-orbit coupling (SOC) is an important and effective way to tune the spin splitting and spin transport by the introduction of space inversion asymmetry. In quantum wells or heterostructures, the SOC is believed to derive from the Dresselhaus term caused by bulk inversion asymmetry (BIA) and the Rashba term resulted from structure inversion asymmetry (SIA) which can be controlled by applying an external electric field.[3-5] The SOC can be regarded as a $\boldsymbol{k}$-dependent effective magnetic field, which causes a spin procession when carriers are transported in a semiconductor. The efficient control of Rashba SOC and its corresponding spin transport via external fields is the core issue in realizing high-performance semiconductor spin devices.

In recent years, the piezotronic and piezo-phototronic effects have been attracting much attention in improving the performance of electronic and optoelectronic devices. These two emerging effects are born characteristics in semiconductor-piezoelectric materials that lack of central symmetry, such as the third-generation wurtzite semiconductors (ZnO, GaN, CdS, etc), transition-metal dichalcogenides (MoS_2, WSe_2, etc), and perovkites.[6-8] So far, they have been widely applied in micro-nano devices, such as transistors[9,10], diodes[11], solar cells[12,13], light emission diodes[14,15] and photodetectors[16,17]. Lately, we have demonstrated experimentally that the piezo-potential, regarded as a "gate" voltage, can be used to effectively tune the Rashba SOC in both P3HT/ZnO nanowire heterostuctures and cation-mixed perovskite nanowires.[18,19] Compared with the piezo-potential, the piezoelectric charges (abbreviated as piezo-charges) at the interfaces or heterostructures can not only tune the SIA or interface electric field as what the piezo-potential does but also induce an in-plane two-dimensional electron gas (2DEG), which may make this kind of manipulation much more efficient due to the confined spin-polarized electrons in the triangular quantum wells. If a circularly polarized light is applied to irradiate on the hetero-interface, the transportation of photo-induced spin-polarized electrons in the triangular quantum wells can be further tuned by the Rashba SOC. However, the study of detailed influence of piezo-charges on Rashba SOC or spin transport has been rarely reported.

In this work, we study theoretically on how the piezo-charges affect the Rashba SOC from a quantitative perspective. Here, organic-inorganic $(CH_3NH_3)PbI_3$ (abbreviated as $MAPbI_3$) is selected as the candidate of p-type material in consideration of that its single-crystal structure possesses a big piezoelectric coefficient. And n-type ZnO thin film with wurtzite structure is used in view of its simple form of Dresselhaus SOC as well as its good piezoelectric property. The large number of positive piezo-charges can attract vast free electrons at the interface of ZnO, forming a high concentration of 2DEG, which can tune the built-in electric field at the interface and further manipulate the Rashba SOC.

From Fig. 1(a), one can see that the *c*-axis directions in the two semiconductor materials are intentionally reversed and point away from the interface. To simplify the calculation, we neglect the lattice mismatch of $MAPbI_3$ and ZnO. When no stress is applied on the devices, there will be space charge regions with positive charges at ZnO side and negative charges at $MAPbI_3$ side. The built-in electric potential energy of n-ZnO/p-$MAPbI_3$ heterojunction can be calculated as $eV_D = E_{Fn}(ZnO) - E_{Fp}(MAPbI_3)$, where e is the electron charge, V_D is the built-in electric potential, E_F is the Fermi energy, respectively. If the electron density is set to be 10^{17}, 10^{16} and 10^{15} cm^{-3}, the Fermi energy E_F is calculated as -4.44, -4.5 and -4.56 eV (see supplementary material for the

detailed calculation). For solution-grown single crystal $MAPbI_3$, a weak p-doped property with a low free hole concentration of ~10^{10} cm^{-3} had been revealed.[20] Here, the Fermi energy E_F of single crystal $MAPbI_3$ was adopted to be -4.8 eV.[20,21] Then, a schematic diagram of energy band of the heterostructure can be plotted, as shown in Fig. 1(b). The inner built-in electric field in ZnO and $MAPbI_3$ can be expressed as

$$E(x) = \frac{qN_D(x-x_n)}{\varepsilon_r(ZnO)\varepsilon_0}, \quad (0 < x < x_n) \qquad (1)$$

$$E(x) = -\frac{qN_A(x-x_p)}{\varepsilon_r(MAPbI_3)\varepsilon_0}, \quad (-x_p < x < 0) \qquad (2)$$

where ε_r, ε_0, x_n and x_p are the relative permittivity, the vacuum permittivity, the width of the space charge region in ZnO, and the width of the space charge region in $MAPbI_3$, respectively. For n^+p junction, one can get $x_p \gg x_n$, and the width of the total space charge region X_D is approximately equal to that in $MAPbI_3$, that is, $X_D \approx x_p$. x_p can be expressed as

$$x_p = \sqrt{\frac{2\varepsilon_r(MAPbI_3)\varepsilon_0 V_D}{qN_A}}, \qquad (3)$$

where $V_D = [E_F(ZnO) - E_F(MAPbI_3)]/e$ = 0.36, 0.3, 0.24 V for electron density of 10^{17}, 10^{16} and 10^{15} cm^{-3}, respectively. Using $\varepsilon_r(MAPbI_3)$ = 9, one can get x_p = 357, 325, 291 μm for electron density of 10^{17}, 10^{16} and 10^{15} cm^{-3}, respectively. According to $x_n = N_A x_p/N_D$, x_n can be obtained as 0.035, 0.325, 2.91 nm for electron density of 10^{17}, 10^{16} and 10^{15} cm^{-3}, respectively, hence they are abrupt hetero-junctions especially for the case of 10^{17} cm^{-3}. The initial maximum value of built-in electric fields E_0 in ZnO (at the interface of $MAPbI_3$/ZnO, i.e., x = 0) are calculated to be -70, -65, -58 V/cm, and Fig. 1(c) shows a schematic distribution of the inner electric field in the p-n^+ junction.

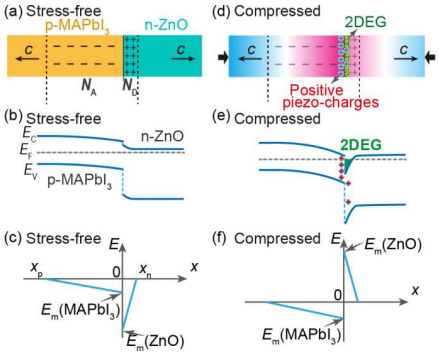

FIG. 1. (a) Schematic diagram of the space charge zone at the interface of p-$MAPbI_3$/n-ZnO. (b) The contact band diagram of the p-$MAPbI_3$/n-ZnO junction without applying compressive pressure. (c) Schematic distribution of the inner electric field in the p-n junction. (d) Energy band diagram when a compressive pressure is applied, denoting the distribution of piezo-potential, positive piezo-charges and 2DEG. (e) The band diagram of the p-n junction when applying a compressive pressure. (f) Schematic distribution of the inner electric field in the p-n junction when applying a compressive pressure.

When a vertical pressure is applied on the devices, there will be positive piezo-charges

induced at the interface, as shown in Fig. 1(d). The piezo-charge density can be expressed as

$$p_{\text{piezo}} = d_{33}\sigma_z, \quad (4)$$

where d_{33} and σ_z are the piezoelectric coefficient and the pressure applied along z-axis, respectively. For ZnO thin film and $MAPbI_3$ single crystal, d_{33} are experimentally measured to be 11.4 pC/N and 31.4 pC/N by former literature, respectively.[22,23] The effective piezo-charge density at the interface of ZnO/$MAPbI_3$ is the sum of positive piezo-charge densities of ZnO and $MAPbI_3$, namely, $p_{\text{piezo}} = [d_{33}(\text{ZnO}) + d_{33}(\text{MAPbI}_3)]\sigma_z = d_{33}^*\sigma_z$, where d_{33}^* is the effective piezoelectric coefficient, and the units of p_{piezo} and σ_z are nC/m^2 and kPa, respectively. Here, the screening effect for piezo-charges due to free carriers in bulk ZnO and $MAPbI_3$ is the driving force of forming 2DEG. The calculated piezo-charge density as a function of pressure is shown in Fig. 2(a).

If applying a 1 MPa compressive pressure on the device (an ideal state), one can estimate that a large positive piezo-charge density of 42.8 μC/m^2 can be induced at the interface. Hence electrons in ZnO will be attracted to screen the positive piezo-charges. Supposing all of the whole positive piezo-charges are screened by electrons attracted from ZnO, there will be a large 2DEG at the hetero-interface (see Figs. 1(e) and 1(f)) with the electron density of 42.8 μC/m^2, which will elicit an equivalent piezoelectric field E_{PE} of 5.4×10^3 V/cm by using equation

$$E_{\text{PE}} = \frac{p_{\text{piezo}}}{\varepsilon_r(\text{ZnO})\varepsilon_0}, \quad (5)$$

where ε_r(ZnO) = 9 is adopted (see Fig. 2(a)). This piezoelectric field is about two orders of magnitude larger than that of the built-in electric field, revealing good potential in tuning interface electric field. For simplicity and considering the ultra-thin width of 2DEG, the 2DEG in ZnO is supposed to locate at x = 0 with the maximum inner electric field. As the direction of piezoelectric field is opposite with that of the inner electric field without applying pressure, a vertical pressure of about 10 kPa is enough to make the total effective electric field to be zero, and the needed pressure is a little bit larger for higher doped ZnO (see Fig. 2(b)). The effective electric field will reverse the sign to positive if further increasing the pressure, as shown in Figs. 1(f) and 2(b).

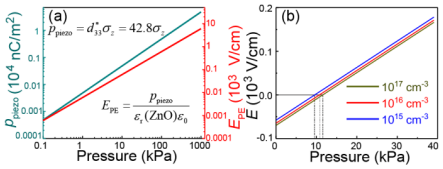

FIG. 2. (a) Piezo-charge density and piezoelectric field as a function of vertical pressure. (b) Effective electric field as a function of vertical pressure when different doping densities in ZnO are adopted.

The Hamiltonian of SOC can be written in the form

$$H_{\text{SO}} = \boldsymbol{\sigma} \cdot \boldsymbol{B}_{\text{eff}}(\boldsymbol{k}), \quad (6)$$

where $\boldsymbol{B}_{\text{eff}}(\boldsymbol{k})$ is an effective magnetic field which is not a real magnetic field hence it can't break the time-reversal symmetry.[24,25] The wurtzite semiconductors with C_{6v} point group is gyrotropic, which allows a $\boldsymbol{k}$-linear spin splitting.[25] Considering the electrons in quantum wells are distributed near the Γ point in the momentum space, the SOC term of 2DEG in wurtzite ZnO grown along

[0001] and with the lattice symmetry of C_{6v} can be expressed as[25-28]

$$H_{SO} = (\alpha + \beta)(\boldsymbol{\sigma} \times \boldsymbol{k})_z = (\alpha + \beta)(\sigma_x k_y - \sigma_y k_x), \qquad (7)$$

where k, α, β, and σ are the electron momentum, the Rashba parameter, the Dresselhaus parameter, and Pauli matrix, respectively. It is to be noted that BIA also results in a $\boldsymbol{k}$-linear spin splitting near the Γ point due to the energy quantization in k_z direction, whose form is strictly the same as that of [111]-grown zinc-blende quantum wells or 2DEG.[25,28] α is in direct proportion to the interface electric field E through the linear relation

$$\alpha = e\alpha_0 E = e\alpha_0(E_{PE} + E_0), \qquad (8)$$

where α_0 is the so-called Rashba coefficient related to the band structure.[29] From the $\mathbf{k}\cdot\mathbf{p}$ theory, α_0 for asymmetric heterostructure is estimated to be proportional to the spin-orbit splitting energy Δ_{so} while inversely proportional to the square of bandgap.[30,31] The value of Δ_{so} for the ZnO 2DEG is unclear. However, the Rashba parameter in ZnO bulk has been calculated to be 1.1 meV Å. We suppose the Rashba value in this ZnO 2DEG to be 1.1 meV Å when no strain is applied on the heterostructure, but actually it should be larger than this value. Then the Rashba coefficients are estimated to be $\alpha_0 = 1.57\times10^3$, 1.69×10^3, 1.9×10^3 Å^2 for ZnO electron densities of 10^{17}, 10^{16} and 10^{15} cm^{-3}, respectively. The pressure dependence of Rashba parameters are calculated, as shown in Fig. 3(a). It can be seen that the Rashba parameters for the three samples are all increased linearly with the increase of vertical pressure, and the value of total Rashba parameter can be wiped out under pressure of 13, 12.1 and 10.8 kPa for ZnO electron densities of 10^{17}, 10^{16} and 10^{15} cm^{-3}, respectively. In other words, it needs more pressure to offset the stronger initial inner electric field in heavily-doped ZnO. The total spin splitting of the energy band resulted from the spin-orbit interaction can be expressed as

$$\Delta E_{SO} = 2k[(e\alpha_0 E_0 + \beta) + \tfrac{e\alpha_0 d^*_{33}}{\varepsilon_r \varepsilon_0}\sigma_z]. \qquad (9)$$

The Rashba and Dresselhaus terms in 2DEG based on wurtzite-type semiconductor can be designed to have opposite signs.[25,27] In the calculation, it is assumed that $\alpha > 0$ and $\beta < 0$ after the 2DEG is formed and that $\alpha < 0$ and $\beta < 0$ before the 2DEG is formed. This assumption may affect the value of the effective piezoelectric coefficient, but the main conclusions of the pressure dependence of SOC should be the same. According to former calculation of this paper, the width of the triangular quantum well in z direction is 0.035, 0.325, 2.91 nm for electron density of 10^{17}, 10^{16}, 10^{15} cm^{-3}, respectively. According to the uncertainty principle, $\Delta z \cdot \Delta k_z \geq 1/2$, and considering the half maximum of the wave function in z direction should be a bit smaller than the width of the triangular quantum well, we suppose $\Delta z \cdot \Delta k_z = 1/\sqrt{2}$. Then one can estimate $k_z \approx \Delta k_z$ to be 2, 0.22 and 0.024 Å^{-1}. And hence the Dresselhaus coefficient β is estimated to be -5400, -64, and -0.75 meV Å for electron density of 10^{17}, 10^{16} and 10^{15} cm^{-3}, respectively, by using $\beta = \gamma b k_z^2$,[27] where γ = 0.33 eV Å^3 and $b \approx 4$. The pressure dependences of the total spin splitting around Γ point, here using $k = 0.03(2\pi/a)$, of conduction band are calculated (where a = 3.25 Å is the in-plane lattice constant of ZnO), as shown in Fig. 3b. The spin splitting for ZnO with electron density of 10^{17} cm^{-3} is relatively large due to the huge Dresselhaus SOC, hence the manipulation of the total SOC by pressure is inefficient. But for ZnO with electron density of 10^{16} cm^{-3}, a 715 kPa pressure can make the spin splitting to be zero. And a much smaller pressure of 18 kPa is enough to wipe out the spin splitting for ZnO with electron density of 10^{15} cm^{-3}. As [0001]-grown wurtzite 2DEGs hold the same configuration as [111]-grown zinc-blende quantum wells or 2DEGs, the electron spin lifetime for ZnO is believed to obey the following expression[32]

$$\tau_x = \tau_y = 2\tau_z \propto (\alpha + \beta)^{-2}. \quad (10)$$

As shown from Fig. 3c, the spin lifetime increases tremendously when the total SOC or spin splitting is gradually vanished, and the manipulation of Rashba SOC by applying pressure can effectively tune the spin lifetime.

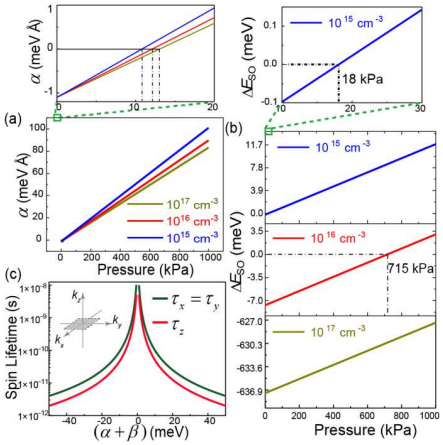

FIG. 3. (a) Pressure dependence of Rashba parameter for different doping densities of ZnO. The upper inset shows an enlarged zone for smaller pressure. (b) Pressure dependence of spin splitting of conduction band for different doping densities of ZnO, and the upper inset shows an enlarged view for pressure ranging from 10 to 30 kPa in the case of 10^{15} cm^{-3}. (c) Spin lifetime as a function of total SOC parameter.

The in-plane effective magnetic field resulted from the spin-orbit interaction can be expressed as

$$\boldsymbol{B}_{\text{eff}} = \left[(e\alpha_0 E_0 + \beta) + \frac{e\alpha_0 d_{33}^2}{\varepsilon_r \varepsilon_0}\sigma_z\right](k_y, -k_x). \quad (11)$$

When the direction of electron spin is parallel to the direction of the effective magnetic field, the energy band of electrons with parallel (or antiparallel) spin direction will split with an increased (or a reduced) energy of $\Delta E_{SO}/2$. $\boldsymbol{B}_{\text{eff}}$ is anticlockwise without applying pressure. The directions of spin-up and spin-down correspond to the directions parallel and antiparallel to $\boldsymbol{B}_{\text{eff}}$, respectively. With the increase of pressure, the $\boldsymbol{B}_{\text{eff}}$ will be reduced to zero and then increased clockwise in the k_x-k_y plane, meanwhile the spin splitting will also be reduced to zero first and then become stronger (see supplementary material Fig. S1). For strong SOC enhanced by pressure, one can use optical methods, such as the circular photogalvanic effect (CPGE) measurement, to realize an efficient spin injection;[3,26,33] and a pressure-gated spin field-effect transistor can also be achieved when the effective magnetic field works at ON and OFF states (see supplementary material Fig. S2).[34]

In conclusion, a piezoelectric p-$MAPbI_3$/n-ZnO heterostructure is studied theoretically. Applying of vertical pressure can induce a large number of positive piezo-charges, which will attract vast electrons at the interface of ZnO, forming a high concentration of 2DEG. The 2DEG can tune the built-in electric field at the interface, and further manipulate the Rashba SOC. With

the increase of pressure, the effective electric field, the Rashba parameter and the spin splitting are all vanished first and then increased linearly for ZnO with doping density of 10^{15} and 10^{16} cm^{-3}. Proper pressures of 18 and 715 kPa for ZnO with doping density of 10^{15} and 10^{16} cm^{-3} are discovered respectively to make the total spin splitting disappearing, resulting in a much longer electron spin relaxation time. The materials selection for this piezotronic effect enhanced SOC should be p-n junction including at least one piezoelectric semiconductor, and the p-n junction should also form a quantum well or 2DEG. The calculation is an ideal case, which may be different with actual measurement because the pressure endurance of the materials and possible interface states, etc., are not taken into consideration. However, this work provides an insight of manipulating electron spins via the introduction of piezo-charges, opening up another cross-cutting research field by combining piezotronics with semiconductor spintronics.

See the supplementary material for the calculation of Fermi energy of ZnO, the schematic diagrams of pressure dependence of the effective magnetic field and spin splitting, and the two application scenarios for pressure-controlled spin injector and spin field transistor.

This research was supported by the National Natural Science Foundation of China (Grant No. 11704032, 51432005, 5151101243, 51561145021), National Key R & D Project from Minister of Science and Technology (2016YFA0202704), Beijing Municipal Science & Technology Commission (Z171100000317001, Z171100002017017, Y3993113DF).

Data Availability Statements

The data that supports the findings of this study are available within the article and its supplementary material.

REFERENCES

[1]D. D. Awschalom and M. E. Flatte, Nat. Phys. **3,** 153 (2007).
[2]A. Manchon, H. C. Koo, J. Nitta, S. M. Frolov, and R. A. Duine, Nat. Mater.s **14,** 871 (2015).
[3]S. Ganichev and W. Prettl, J. Phys-Condens. Mat. **15,** R935 (2003).
[4]G. Dresselhaus, Phys. Rep. **100,** 580 (1955).
[5]E. I. Rashba, Sov. Phys. Solid State **2,** 1109 (1960).
[6]Z. L. Wang, Adv. Mater. **24,** 4632 (2012).
[7]Z. L. Wang, Nano Today **5,** 540 (2010).
[8]Z. L. Wang, Mater. Today **10,** 20 (2007).
[9]L. Wang, S. Liu, G. Gao, Y. Pang, X. Yin, X. Feng, L. Zhu, Y. Bai, L. Chen, T. Xiao, X. Wang, Y. Qin, and Z. L. Wang, ACS Nano **12,** 4903 (2018).
[10]W. Wu, X. Wen, and Z. L. Wang, Science **340,** 952 (2013).
[11]J. Zhou, P. Fei, Y. Gu, W. Mai, Y. Gao, R. Yang, G. Bao, and Z. L. Wang, Nano Lett. **8,** 3973 (2008).
[12]L. Zhu and Z. L. Wang, Adv. Funct. Mater. **29,** 1808214 (2019).
[13]L. Zhu, L. Wang, F. Xue, L. Chen, J. Fu, X. Feng, T. Li, and Z. L. Wang, Adv. Sci. **4,** 1600185 (2017).
[14]M. Chen, C. Pan, T. Zhang, X. Li, R. Liang, and Z. L. Wang, ACS Nano **10,** 6074 (2016).
[15]X. Li, M. Chen, R. Yu, T. Zhang, D. Song, R. Liang, Q. Zhang, S. Cheng, L. Dong, A. Pan, L. Wang

Zhong, J. Zhu, and C. Pan, Adv. Mater. **27,** 4447 (2015).
[16]P. Lin, L. Zhu, D. Li, L. Xu, C. Pan, and Z. Wang, Adv. Funct. Mater. **28,** 1802849 (2018).
[17]Q. Lai, L. Zhu, Y. Pang, L. Xu, J. Chen, Z. Ren, J. Luo, L. Wang, L. Chen, K. Han, P. Lin, D. Li, S. Lin, B. Chen, C. Pan, and Z. L. Wang, ACS Nano **12,** 10501 (2018).
[18]L. Zhu, Y. Zhang, P. Lin, Y. Wang, L. Yang, L. Chen, L. Wang, B. Chen, and Z. L. Wang, ACS Nano **12,** 1811 (2018).
[19]L. Zhu, Q. Lai, W. Zhai, B. Chen, and Z. L. Wang, Mater. Today (2020). https://doi.org/10.1016/j.mattod.2020.02.018
[20]Q. Dong, Y. Fang, Y. Shao, P. Mulligan, J. Qiu, L. Cao, and J. Huang, Science **347,** 967 (2015).
[21]P. Cui, D. Wei, J. Ji, H. Huang, E. Jia, S. Dou, T. Wang, W. Wang, and M. Li, Nat. Energy **4,** 150 (2019).
[22]X. B. Wang, C. Song, D. M. Li, K. W. Geng, F. Zeng, and F. Pan, Appl. Surf. Sci. **253,** 1639 (2006).
[23]S. Liu, F. Zheng, I. Grinberg, and A. M. Rappe, J. Phys. Chem. Lett. **7,** 1460 (2016).
[24]P. S. Eldridge, W. J. H. Leyland, P. G. Lagoudakis, O. Z. Karimov, M. Henini, D. Taylor, R. T. Phillips, and R. T. Harley, Phys. Rev. B **77,** 125344 (2008).
[25]S. D. Ganichev and L. E. Golub, Phys. Status Solidi B **251,** 1801 (2014).
[26]C. Yin, B. Shen, Q. Zhang, F. Xu, N. Tang, L. Cen, X. Wang, Y. Chen, and J. Yu, Appl. Phys. Lett. **97,** 181904 (2010).
[27]J. Y. Fu and M. W. Wu, J. Appl. Phys. **104,** 093712 (2008).
[28]R. Eppenga and M. F. H. Schuurmans, Phys. Rev. B **37,** 10923 (1988).
[29]M. A. Leontiadou, K. L. Litvinenko, A. M. Gilbertson, C. R. Pidgeon, W. R. Branford, L. F. Cohen, M. Fearn, T. Ashley, M. T. Emeny, B. N. Murdin, and S. K. Clowes, J. Phys-Condens. Mat. **23,** 035801 (2011).
[30]E. A. de Andrada e Silva, G. C. La Rocca, and F. Bassani, Phys. Rev. B **50,** 8523 (1994).
[31]F. G. Pikus and G. E. Pikus, Phys. Rev. B **51,** 16928 (1995).
[32]X. Cartoixà, D. Z. Y. Ting, and Y. C. Chang, Phys. Rev. B **71,** 045313 (2005).
[33]Q. Zhang, X. Wang, C. Yin, F. Xu, N. Tang, B. Shen, Y. Chen, K. Chang, W. Ge, and Y. Ishitani, Appl. Phys. Lett. **97,** 041907 (2010).
[34]I. Žutić, J. Fabian, and S. Das Sarma, Rev. Mod. Phys. **76,** 323 (2004).

PLEASE CITE THIS ARTICLE AS DOI: 10.1063/5.0011280

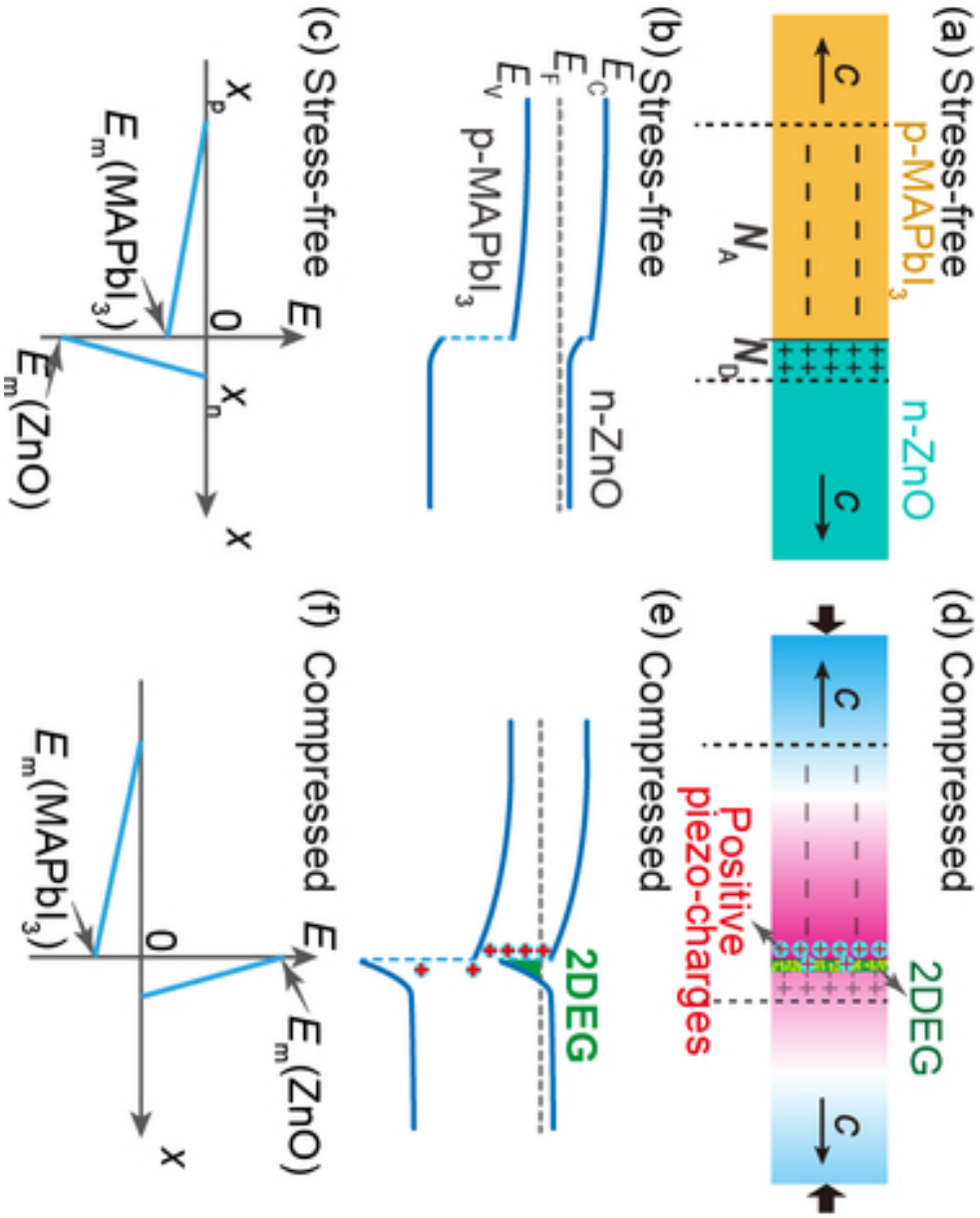

PLEASE CITE THIS ARTICLE AS DOI: 10.1063/5.0011280